

Closing the spin gap of $(\text{NH}_4)_x\text{K}_{1-x}\text{CuCl}_3$ through chemical substitutionJared S. Kinyon^{⊗,*}, N. S. Dalal[†] and R. J. Clark[‡]*Department of Chemistry and Biochemistry, Florida State University, Tallahassee, Florida 32306-4390, USA*Haidong Zhou[⊗]*Department of Physics and Astronomy, The University of Tennessee, 401 Nielsen Physics Building, Knoxville, Tennessee 37996, USA*K. Y. Choi[§]*Department of Physics, Sungkyunkwan University, Suwon, Korea*

(Received 25 January 2021; accepted 27 April 2021; published 24 May 2021)

Unlike potassium trichlorocuprate KCuCl_3 , the isostructural ammonium trichlorocuprate NH_4CuCl_3 exhibits the rather unusual effect of orientation-independent steps in the magnetization (M) as a function of the applied magnetic field (H). However, replacement of NH_4^+ by the isomeric K^+ ion results in a smearing of these steps. With the view of probing this change, we carried out on the mixed system $(\text{NH}_4)_x\text{K}_{1-x}\text{CuCl}_3$, with $x = 0.0, 0.3, 0.6, 0.9$, and 1.0 : (1) High-field pulsed measurements of M versus H at 1.5 K, (2) susceptibility measurements from 1.8 to 295 K and (3) zero-field specific heat measurements from 1.8 to 295 K. The magnetization steps were found to be highly sensitive to the NH_4^+ ion concentration, with the spin gap Δ generally decreasing with increasing x . Analysis of the susceptibility and specific heat data with several theoretical schemes also supports this general trend. This includes data analysis using the Bleaney-Bowers, Ising chain, and the mean-field model. These results yielded intradimer spin-exchange constants of the order of 20 – 40 K, somewhat smaller than expected for $\text{Cu}^{2+} - \text{Cu}^{2+}$. This, in addition to the variation of x with Δ , points to the need for additional theoretical modeling.

DOI: [10.1103/PhysRevMaterials.5.054413](https://doi.org/10.1103/PhysRevMaterials.5.054413)

I. INTRODUCTION

NH_4CuCl_3 , henceforth labeled ACC, has been a compound of interest for quite some time, in particular for its multiferroic properties. It has been found to possess a ferroelectric transition at 67 K [1] and exhibits magnetoelectric behavior below the antiferromagnetic transition at 1.3 K [2]. Its magnetic properties began to be studied more intensely when Shiramura and colleagues discovered magnetization plateaus at $\frac{1}{4}$ and $\frac{3}{4}$ of the saturation moment that occurred independently of the direction of the applied field [3]. This led them to conclude that the plateaus could be described in terms of a quantum many-body effect, not originating from a metamagnetic transition or zero-field splitting.

The room-temperature space group of ACC is $P2_1/c$, and the CuCl_3^- groups occur as alternating chains along the a axis [4,5]. This makes it amenable to study as a spin $\frac{1}{2}$ alternating Heisenberg chain with nearest-neighbor interactions [6–8]. However, this model did not predict the expected plateau positions, so it was assumed that the formation of a magnetic superstructure was responsible for the plateaus. Another possibility was suggested by Matsumoto, that is, the inequivalent Cu^{2+} sites came from a structural phase transition [9]; this has been consistently observed at 70 K through the use of IR

spectroscopy [10], ultrasonic attenuation [11,12], ^{15}N -NMR [13], ^{14}N -NMR [14], and neutron diffraction [15].

But the coupling problem still remains unsolved, considering the neutron diffraction [15–17], NMR [13,14,18–20], EPR [21,22], and heat capacity [23] results. Four of the eight Cu^{2+} ions in the low-temperature phase should be unique. However, the quadrupole splitting in ^{14}N -NMR has shown that the inversion symmetry of the low-temperature phase ($P\bar{1}$) is lost below 70 K, which makes locating the polarized spins rather difficult [18]. It is very likely that interchain interactions play an important role in the coupling scheme, making them necessary for understanding the plateaus.

Initially, it was not well understood why the theoretically more robust spin $\frac{1}{2}$ plateau was not observed [3,6,7,9]; fortunately, the aforementioned structural studies have shown that the plateau positions originate from different dimers. The point of interest at this juncture is to find out how the dimers couple. Whatever model is used must also be compatible with the 3D antiferromagnetic ordering below 1.3 K [13,16,18,22].

Like ACC, KCuCl_3 (KCC) has the same space group and the chain structure, making it an isostructural compound at room temperature [4,5,15]. Moreover, there is no reported structural phase transition. This is not surprising, given that the low 70 -K transition is likely related the reorientational movement of the ammonium ions [1]. Additionally, the magnetic properties of both compounds are very different, despite their structural similarities. We believe doping ACC with K^+ would provide for an interesting magnetic system to study, for the reasons outlined below.

*jaredkinyon@gmail.com

†ndalal@fsu.edu

‡clark@chem.fsu.edu

§choisky99@skku.edu

First, the ground state of KCC has a definite excitation gap, which has been demonstrated with susceptibility [24], magnetization [25], neutron diffraction [26–36], and ESR measurements [37]. Subsequent analyses of the dispersion relation led to the conclusion that the spin dimers were only marginally coupled [28,38]. Clearly, the structural phase transitions of ACC led it to behave quite differently from KCC at low temperatures. It would be of high interest to know the extent to which potassium ion substitution could suppress this transition; if suppression of the transition occurs with even slight potassium substitution, one could track changes in magnetism due to ion concentration alone.

This study would also be interesting, as only a limited amount of work has been carried out on mixed variants of the trichlorocuprates. More specifically, μ SR [39] and magnetization [40] measurements have been made on $Tl_xK_{1-x}CuCl_3$ in order to understand the role of random bond effects on the ground state. These were particularly useful, as $TlCuCl_3$ shows evidence of strong interdimer coupling [41–45], whereas $KCuCl_3$ does not [29–31]. Both studies show that mixing the two ions results in a magnetic (as opposed to a singlet) ground state [37], and that a frozen state may exist near a potassium concentration of 0.6 [38]. A similar frozen state has been hypothesized from μ SR measurements with replacing the copper(II) ion with Mg, i.e., $KCu_{1-x}Mg_xCl_3$ [39,46].

II. EXPERIMENTAL METHODS

NH_4CuCl_3 was synthesized according to the standard procedures [3–5]. Specifically, equimolar amounts of NH_4Cl and anhydrous $CuCl_2$ were slowly dissolved in absolute ethanol in a dry nitrogen atmosphere, followed by slow evaporation at 333 K. The result was a set of dark red needles, which upon careful examination with a polarizing microscope was found to be untwinned. The authenticity of this compound was verified with single-crystal x-ray diffraction down to 100 K, and the unit-cell dimensions precisely matched all those found in the literature.

The literature for the solution-based synthesis of $KCuCl_3$ is quite scant when compared to the aforementioned compounds, as most other authors relied on the Bridgman technique to grow large crystals. The method cited by Willet *et al.* [4] is that of Groger [47], whereas a concentrated HCl solution is saturated with a 1:2 molar ratio of $CuCl_2 \cdot 2H_2O$ to KCl and then allowed to evaporate over $Mg(ClO_4)_2$. Due to the inherent risks of dealing with perchlorates, another method was devised. A 1:1 molar ratio of KCl: $CuCl_2$ was dissolved into a solution of CH_3CN and slowly allowed to evaporate at 333 K under dry conditions. Like ACC, these crystals grew as long needles with a red or yellow green color depending upon the angle in which it was viewed under a polarizing microscope.

Samples of $[(NH_4)_xK_{1-x}]CuCl_3$ were grown in a manner very similar to that of KCC. A measured amount of KCl salt was slowly dissolved into a warm acetonitrile solution with constant stirring until saturation was achieved. The same procedure was separately carried out with NH_4Cl and anhydrous $CuCl_2$ in their own respective CH_3CN solutions. Given the initial concentration of each solution, the appropriate amount

of each solution was added together such that the molar ratio of each component ($CuCl_2:NH_4Cl:KCl$) was 1: x : $1-x$. The final solution was then kept at 333 K in a warm heating bath and allowed to slowly evaporate. The crystals took on the same appearance as the original compounds, i.e., long reddish needles [48].

During crystallography work, single mm-sized crystals were cut from large samples and mounted on a nylon loop with the use of heavy oil, typically Paratone-N. The samples were typically held at low temperatures for data collection, which protects them from moisture. Full data were taken on a Bruker SMART APEX II diffractometer equipped with a graphite monochromator and $Mo\ K\alpha$ ($\lambda = 0.71073\ \text{\AA}$) radiation source lying 6 cm from the CCD detector. The number of frames taken was typically 2400 using 0.3 degree omega scans with 20 seconds of frame collection time. Integration was performed using the program SAINT, which is part of the Bruker suite of programs. Absorption corrections were made using SADABS. XPREP was used to obtain an indication of the space group and the structure was typically solved by direct methods and refined by SHELXTL. The non-hydrogen atoms were refined anisotropically. Typically the hydrogen atoms could be found during the least-squares refinement, but in practice they are constrained as a riding model. If disorder was present, every effort was made to model it.

Variable-temperature magnetic susceptibility (χ) measurements on various powdered and single crystal ammonium/potassium mixtures ($x = 0.0, 0.3, 0.5, 0.9, 1.0$) were carried out from 1.8 to 300 K on the RSO transport of an Quantum Design MPMS XL magnetometer using an applied field of 100–500 G, depending upon the sensitivity of the sample. For the same series, specific heat (C_p) measurements of single crystal samples were made with zero magnetic field from 1.8 to 200 K using the heat capacity option from Quantum Design's Model 6000 Physical Property Measurement System, which employs the time-constant method. Samples were mounted on the puck platforms with Apiezon N grease along the long-edge faces of the crystal to provide better sample coupling. High-field magnetization was measured with a pulsed-field magnet at the Dresden High Magnetic Field Laboratory. The magnetic moment was sensed by a standard inductive method with a pick-up coil technique in the field range of $\mu_0 H = 0\text{--}60\ T$.

III. RESULTS AND DISCUSSION

A. X-ray Structure

When two atoms occupy the same position, a variation in the standard procedure to obtain an initial solution might be required. For instance, in the case of a mixture of ammonium and potassium ions, the average electron count that the x-rays see is neither 7 nor 19. The structure solution was often easiest if a fake atom with a Z value somewhere between was used in the preliminary efforts. Then, to obtain the best ratio, the two elements were entered into the instruction file with the same position. Commands were used to force them to have the same positions and equal atomic displacement parameters. Finally, the PART command was used followed by cycles of least squares to obtain the best ratio of two ions. A comparison

TABLE I. A comparison of unit-cell information for mixed variants of $[(\text{NH}_4)_x\text{K}_{1-x}]\text{CuCl}_3$ from $x = 1$ to $x = 0$. All crystals were almost of identical unit-cell composition, belonging to the monoclinic crystal system and $P2_1/c$ space group at room temperature.

x	1	0.9	0.5	0.30	0
F.W. (g/mol)	187.93	190.23	198.46	202.68	209.00
a (Å)	4.028	4.033	4.022	4.025	4.010
b (Å)	14.183	14.288	13.999	13.911	13.764
c (Å)	8.980	9.037	8.856	8.793	8.704
β (deg)	96.35	95.68	96.55	96.55	96.86
Volume (Å ³)	509.84	518.20	495.42	489.05	476.93

of the unit cell parameters at room temperature for the various ions can be found in Table I. As expected, no significant change was found for any of the parameters with a change in composition.

B. Magnetization

The field-derivative magnetization curves measured at 1.5 K for various mixtures and orientations of $[(\text{NH}_4)_x\text{K}_{1-x}]\text{CuCl}_3$ ($x = 0.3, 0.5, 0.9$) are presented in Fig. 1. In all cases, the magnetization increases monotonically with the magnetic field, with at least one continuous transition being found before saturation. Unfortunately, due to problems with the magnet, the maximum field could not be achieved for all compositions. The field transitions H_c are all associated with saturation or the spin gap $\Delta = g\mu_B H_c$, and are most clearly observed as anomalies in the $\frac{dM}{dH}$ curve. These results are presented in Table II. The relative broadness of the powdered sample transitions is likely due to g anisotropy, as has been observed for KCC [25] and ACC [3]. For the compositions $x = 0.3, 0.5$, and 0.9 , the respective critical fields are $H_{c1} = 19.6, 13.7$, and 5.7 T. All of these values are less than the gap found for KCC at 23 T ($\Delta = 31$ K) [25], and decrease with decreasing K^+ concentration. Given that ACC

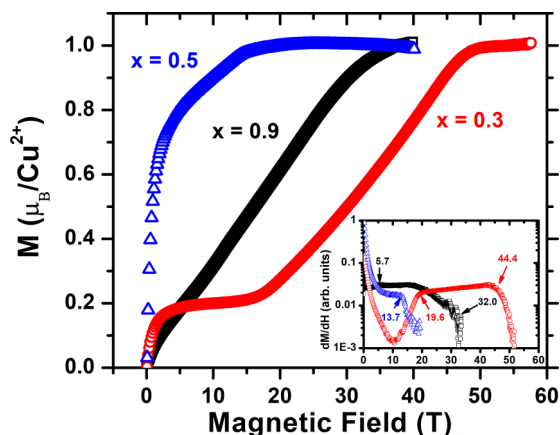


FIG. 1. Magnetization as a function of the applied magnetic field for $[(\text{NH}_4)_x\text{K}_{1-x}]\text{CuCl}_3$ at 1.5 K when $x = 0.9$ (black squares), 0.5 (blue triangles), and 0.30 (red circle). The inset depicts the field-derivative magnetization, with the y axis on a logarithmic scale in order to properly scale the different magnitudes and clarify the critical field positions as a function of field.

TABLE II. Critical field(s) and estimated spin gap at 1.5 K for various compositions of $[(\text{NH}_4)_x\text{K}_{1-x}]\text{CuCl}_3$. The estimate for $\Delta = g\mu_B H_c$ when $0 < x < 1$ was obtained using H_{c1} and by assuming $g = 2$. Values for $x = 0$ were obtained from the literature [25].

x	Orientation	H_{c1} (T)	H_{c2} (T)	Δ (K)
0	[201]	23	54	31
0.3	[100]	19.6	44.4	26
0.5	powder	13.7		18
0.9	powder	5.7	32.0	7.7

is a gapless compound ($\Delta = 0$), these results strongly suggest that Δ can be fine tuned in the full range from 31 to 0 K by precisely controlling the potassium ion concentration. EPR measurements were not considered to be necessary because an estimate of Δ could be made by assuming that $g \approx 2$, which is reasonable given that single crystal measurements showed variations from 2.06 to 2.17 for ACC [21] and 2.04 to 2.26 for KCC [25].

C. Magnetic Susceptibility

The original susceptibility for $[(\text{NH}_4)_x\text{K}_{1-x}]\text{CuCl}_3$ when $x = 0, 0.3, 0.5$, and 0.9 along the long, crystallographic a axis is shown in Fig. 2. Orphan spins, likely generated from chemical disorder [49,50], produced a significant Curie tail at low temperatures. This effect was accounted for by fitting the inverse susceptibility to the Curie-Weiss law ($\frac{1}{\chi} = \frac{T-\Theta}{C}$) in a narrow temperature range. A paramagnetic curve over the entire temperature range was then produced from parameters Θ and C , which was then subtracted from the original data. These parameters are listed for each composition in Table III.

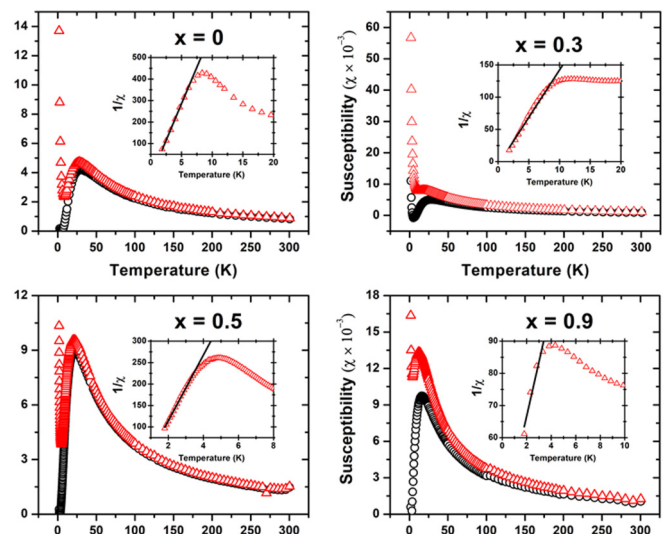


FIG. 2. The original magnetic susceptibility data for $[(\text{NH}_4)_x\text{K}_{1-x}]\text{CuCl}_3$ along the a axis when $x = 0, 0.3, 0.5$, and 0.9 is presented with red triangles; when corrected for paramagnetic impurities, the susceptibility is presented with black circles. The inset provides a closer view of the inverse susceptibility, with a best fit line being used to determine the paramagnetic impurity.

TABLE III. Fitting parameters for the magnetic susceptibility of various concentrations of $[(\text{NH}_4)_x\text{K}_{1-x}]\text{CuCl}_3$. Parameters J (K) and J' (K) respectively refer to intra and interdimer coupling constants, while g holds its usual meaning. Spin-gap energies Δ (K) are also estimated based off of the Troyer estimate and the susceptibility models using Eq. (4). Both Θ (K) and C correspond with the constants used to construct a Curie curve and correct for the increased moment produced by orphan spins.

x	Troyer	Ising chain				Mean-field				B-Bowers		Orphan spins	
	Δ_T	J_I	J'_I	g_I	Δ_I	J_M	J'_M	g_M	Δ_M	J_B	g_B	C	Θ
0	35.7(8)	-37.3(1)	6.41(8)	1.67(1)	30.2	-45.8(1)	0.17(1)	1.52(1)	45.6	-48.3(2)	1.17(1)	7.34×10^{-3}	0.83
0.30	27.5(2)	-32.7(1)	3.3(1)	2.02(1)	29.9	-35.9(1)	0.37(1)	1.61(1)	35.5	-40.1(1)	1.37(1)	1.90×10^{-2}	0.69
0.50	19.7(1)	-27.3(1)	-0.1(4)	2.16(1)	27.3	-26.5(1)	0.55(1)	1.46(1)	25.9	-32.3(2)	1.41(1)	1.31×10^{-2}	0.50
0.90	13.9(4)	-20.2(1)	-0.6(5)	1.97(1)	20.8	-19.3(2)	0.57(1)	1.30(1)	18.7	-25.0(2)	1.30(1)	5.94×10^{-2}	-2.0

A direct comparison of the corrected susceptibilities is given in Fig. 3. There is a gradual decrease in the peak temperature T_{max} and width with decreasing K^+ concentration, with respective values of 29, 25, 21, and 16 K for $x = 0, 0.3, 0.5,$ and 0.9. The susceptibility for $x = 1$ is not shown, as no local maximum was observed; this could be due to the smaller fields we used (500 Oe) as compared to the literature (10,000 Oe) [3].

It has been shown that for KCC, intranuclear interactions are the most dominant magnetic interaction [38]. Thus, in order to model the susceptibility for the $[(\text{NH}_4)_x\text{K}_{1-x}]\text{CuCl}_3$ series, it seemed most prudent to begin with the simplest dinuclear cluster approximation, given by the Bleaney-Bowers formula [51]

$$\chi = \frac{2N_A(g\mu_B)^2}{k_B T (3 + e^{J/k_B T})}, \quad (1)$$

where N_A is Avogadro's number, g is the electronic g value, μ_B is the Bohr magneton, k_B is Boltzmann's constant, and J is the intradimer exchange integral. The best fit parameters g_B and J_B for each composition are listed in Table III, and the resulting curve for each composition is displayed in Fig. 4.

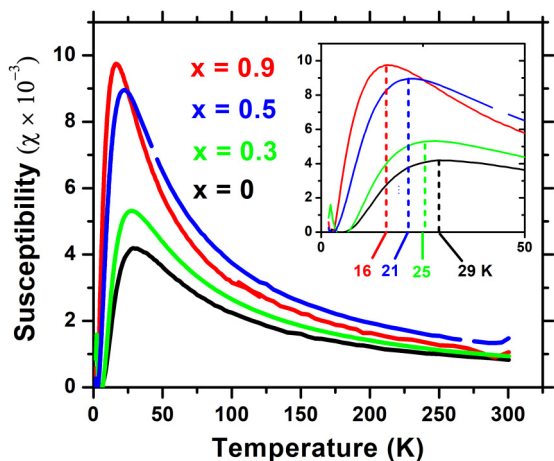


FIG. 3. Temperature dependence of the magnetic susceptibility for $[(\text{NH}_4)_x\text{K}_{1-x}]\text{CuCl}_3$ when $x = 0$ (black), 0.3 (green), 0.5 (blue), and 0.9 (red); the curves have all been corrected for paramagnetic impurities as described in text. The inset provides a closer view of T_{max} from 0 to 50 K.

However, $g_B \ll 2$ for all compositions, which suggests that the experimental susceptibility is less than what is predicted by this model. Additionally, the applied fit is slightly smaller than the experimental data in the range from $T_{\text{max}} < T < 300$ K for $x = 0.3, 0.5,$ and 0.9. Thus, it is necessary to account for the interdimer interactions to properly model the magnetic susceptibility over the entire temperature range. One such approach, referred to as the mean-field model, assumes an average interdimer interaction $J' \ll J$ [52,53]. The susceptibility in this case is given by

$$\chi = \frac{2N_A(g\mu_B)^2}{k_B T (3 + e^{\Delta/k_B T} - J'/T)}. \quad (2)$$

Use of this formula provided a more satisfactory fitting to the susceptibility over the entire temperature range, covering even the higher temperatures that the Bleaney-Bowers model could not. However, the g values were still too small. So we used another approach for modeling the interdimer interactions and started viewing the system as an Ising

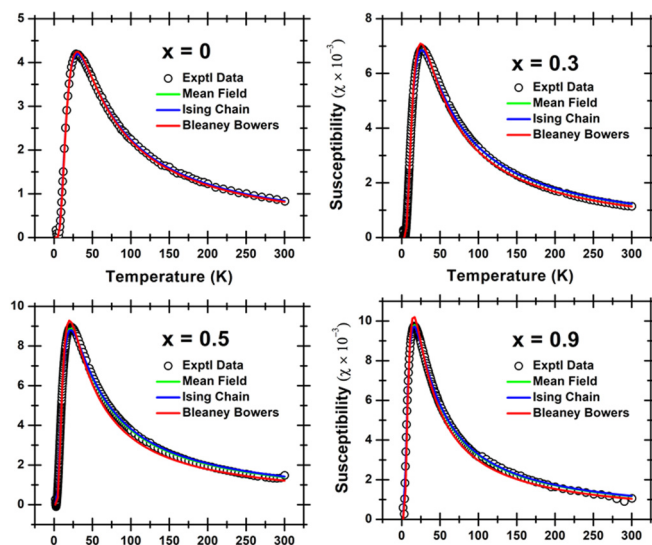


FIG. 4. A comparison of the mean field (green line), Ising chain (blue line), and Bleaney-Bowers (red line) models used to fit the susceptibility of $[(\text{NH}_4)_x\text{K}_{1-x}]\text{CuCl}_3$ for $x = 0, 0.3, 0.5,$ and 0.9. All models fit quite nicely to the susceptibility, creating significant overlap between the lines over the entire temperature range. This makes distinguishing between the fits quite difficult. The parameters for each fit are listed in Table III.

spin chain. This perspective is depicted in Fig. 5, which shows the arrangement of Cu^{2+} ions into $\text{Cu}_2\text{Cl}_6^{2-}$ chains for KCC.

$$\mathcal{H} = -2JS_m^z S_n^z - 2J'(S_m^z S_{m+1}^z + S_n^z S_{n+1}^z) - g\beta H(S_m^z + S_n^z), \quad (3a)$$

$$\chi = \frac{Ng^2\beta^2}{4kT} \left[\frac{e^{2K'}(e^{KR} - \sinh 2K')}{(R - e^K \sinh 2K')(\cosh^2 K \cosh^2 2K' - \sinh^2 2K')^{1/2}} \right], \quad (3b)$$

$$R = \cosh K \cosh 2K' + (\cosh^2 K \cosh^2 2K' - \sinh^2 2K')^{1/2}, \quad (3c)$$

where $K = J/2k_B T$ and $K' = J'/2k_B T$. As shown in Fig. 4, the fit for the Ising chain model practically overlaps with mean-field curve; however, the parameters for g for the mixed-ion compositions are closer to what is expected for a Cu^{2+} ion.

In addition to modeling the susceptibility, we thought it would be of interest to estimate the spin gap Δ from the fit susceptibility. Oosawa *et al.* have already shown that for KCC, Δ can be estimated from the coupling constants J and J' [25]:

$$g\mu_B H_c = \sqrt{J^2 + 2JJ'}. \quad (4)$$

This formula was derived from the calculation of the magnetization curve of a spin dimer at $T = 0$ with a mean-field model, assuming that triplet excitations are created on the dimer site. In order to use this formula, we had to treat both J'_I and J'_M as an average interdimer interaction, despite this not being strictly true for J'_I . The various estimates for Δ based on these assumptions are given in Table III. As a final check, an estimate for Δ based on the low-temperature susceptibility has been suggested by Troyer, who used a Lanczos algorithm to calculate the susceptibility based on an antiferromagnetic Heisenberg ladder system [54]. Such an approach has already been shown to be applicable to KCC [24], with $\chi \propto \frac{1}{\sqrt{T}} e^{-\frac{\Delta}{k_B T}}$ at low temperatures, below T_{\max} . This fitting was applied to various mixed compositions from 4 to 15 K and can be found below in Fig. 6.

D. Heat Capacity

Figure 7 displays the temperature dependence of $\frac{C_p}{T}$ for all of the compositions from $x = 0$ to $x = 0.9$. Temperature

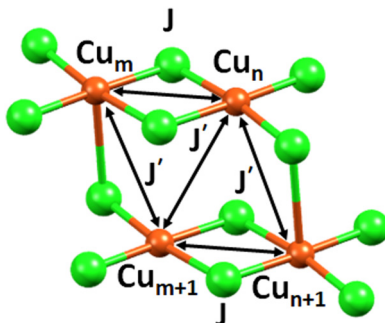


FIG. 5. Illustration of the proposed magnetic coupling scheme for the mixed trichlorocuprates. Here, the Cu^{2+} ions (red) are coupled in $\text{Cu}_2\text{Cl}_6^{2-}$ chains, with J and J' , respectively, representing the intradimer and interdimer coupling constants.

If one disregards the interaction between S_n and S_{m+1} , one can derive a rigorous formula for the parallel susceptibility based on the Hamiltonian given by Eq. (3a) [53]:

dependent C_p data for ACC showing the two structural phase transitions has already been published [1]. In the full temperature range from 1.8 to 200 K, no structural phase transition could be found. However, a change in slope associated with the spin gap was observed at low temperatures in the original $C_p(T)$ data, which has been observed in the isostructural TlCuCl_3 [55]. When $H = 0$, it was shown that for the gap contribution to the specific heat, $C_p \propto e^{-\frac{\Delta}{T}}$. This relationship is best clarified by plotting the temperature dependence of $\frac{C_p}{T}$, with the slope change manifesting as a local maximum centered at Δ .

In order to model the specific heat for all compositions, we assumed that the only two contributions to C_p are from the lattice and the aforementioned gap contribution. This represented below with the sum of a Debye oscillator and an exponential term:

$$C_p = \left(C_D \frac{T^3}{\Theta_D^3} \int_0^{\Theta_D/T} \frac{x^4 e^x dx}{(e^x - 1)^2} \right) + C_g e^{-\Delta/T}. \quad (5)$$

Here C_D and C_g are, respectively, constants of proportionality for the lattice and gap terms, Θ_D is the Debye temperature, and Δ is the gap energy. The resulting fit and individual contributions from each term to $\frac{C_p}{T}$ for each composition is depicted in Fig. 7, with the parameters for each fit being listed

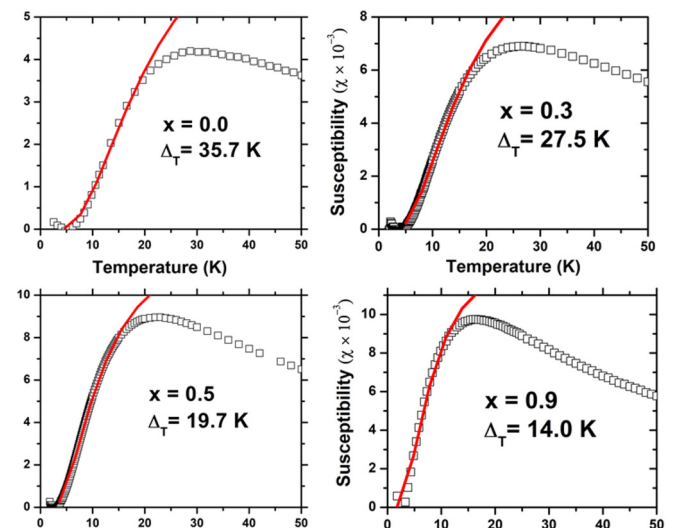


FIG. 6. Low-temperature fits of the susceptibility based on the Troyer estimates for various compositions of $[(\text{NH}_4)_x\text{K}_{1-x}]\text{CuCl}_3$.

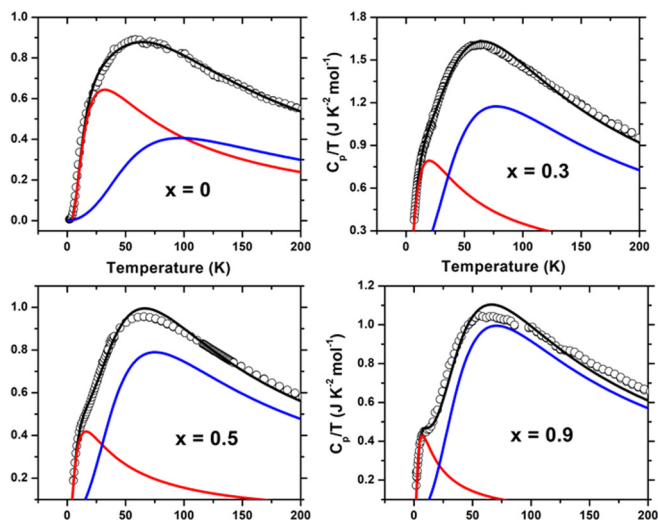


FIG. 7. A fitting of the temperature dependence of $\frac{C_p}{T}$ for all compositions using Eq. (5). The black curves represents the total heat specific heat, while the blue and red curves represent the contributions from the lattice and gap energy, respectively.

in Table IV. For KCC, the gap energy was set to the known $\Delta = 31$ K.

As expected from the aforementioned susceptibility and magnetization results, Δ , and by extension the peak, shifted to higher temperatures with increasing K^+ concentration. Though the trend is clear, it is important to keep in mind that it is not an accurate quantitative indicator of Δ as magnetization since the gap contribution becomes increasingly difficult to deconvolute from the increasingly dominant lattice component at higher temperatures.

Another interesting trend from the C_p data can be observed in Fig. 8, which displays the temperature dependence of $\frac{C_p}{T^3}$ for all compositions. Here, one can see the gradual formation of a peak with increasing K^+ concentration, with a fully centered peak (9.4 K) being fully visible only for KCC. Such a signature signifies a specific heat in excess of what is predicted by the Debye model at low temperatures, often arising from some kind of structurally glassy state due to local ordering [56–58]. Specifically, this is often ascribed to factors like localized vibrations, domain wall motions, and transverse phonon modes in a variety of different materials [59–61], one notable crystalline example being $Ba_2Ti_2O_7$ [57]. For the mixed trichlorocuprates, it quickly became apparent that KCC possessed the largest disorder and most glassy behavior since it had the sharpest and most visible peak. The trend of the peak dissipating with increasing NH_4^+ concentration

TABLE IV. Parameters found using a least squared fitting of $\frac{C_p}{T}$ for $[(NH_4)_xK_{1-x}]CuCl_3$ using Eq. (5) from 1.8 to 200 K.

x	$C_D(\frac{J}{K\text{-mol}})$	$\Theta_D(K)$	$C_g(\frac{J}{K\text{-mol}})$	$\Delta(K)$
0	207(3)	346(6)	56.0(7)	31
0.30	478(2)	276(1)	42.7(5)	19.8(1)
0.50	313(1)	268(1)	18.1(4)	16.0(2)
0.90	370(3)	252(2)	8.3(3)	7.1(2)

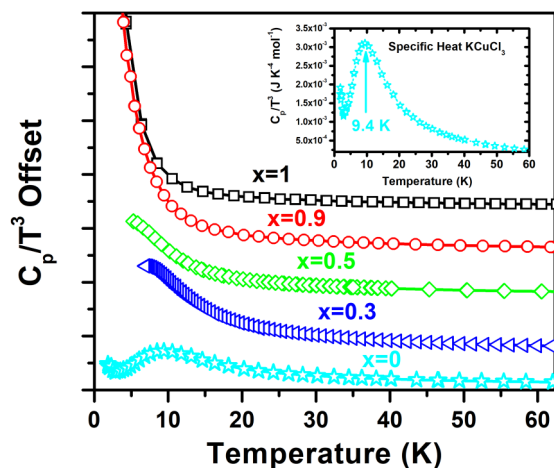


FIG. 8. Temperature dependence of $\frac{C_p}{T^3}$. Here, the plot clearly shows a series of peaks related to some kind of glassy transition. Peaks are staggered for easy comparison. The inset magnifies the peak for $KCuCl_3$, which is centered at 9.4 K.

is likely related to the configuration of spin centers since ACC is known to possess two structural phase transitions and long-range antiferromagnetic ordering, all of which KCC does not possess. This idea is also supported by temperature dependent Raman experiments on KCC, which have shown that delocalized triplets are responsible for modulating lattice dynamics through spin-lattice interactions [62]. Similar Raman results have also been found in the gapped isostructural series $K_xTl_{1-x}Cl_3$ [63].

IV. CONCLUSIONS

A comparison of all the calculated gap energies for various compositions of $[(NH_4)_xK_{1-x}]CuCl_3$ is depicted in Fig. 9. All techniques generally follow the trend of a decreasing spin gap Δ with increasing NH_4^+ ion concentration, with the calculations based on the Troyer estimate and pulsed

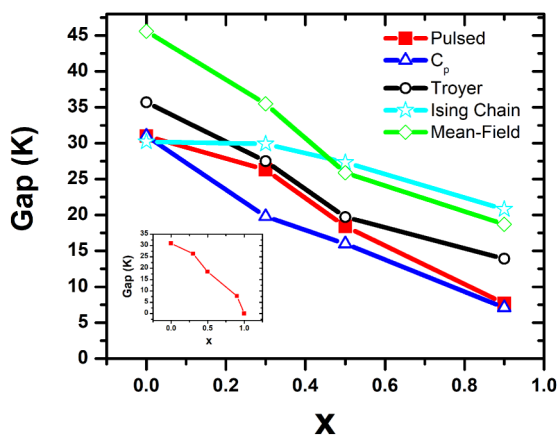


FIG. 9. A comparison of the gap energy for compositions of $[(NH_4)_xK_{1-x}]CuCl_3$ calculated through magnetization, magnetic susceptibility (Troyer, Ising chain and mean-field), and specific heat measurements. The inset displays Δ calculated through magnetization alone in order to clearly depict the overall trend.

magnetization technique being the most self-consistent across the entire range of x . Given that ACC ($x = 1$) is gapless, the inset of Fig. 9 clearly shows that the magnitude of Δ is much more sensitive to doping when $0.9 < x < 1$.

Since there was no observation of a structural phase transition through C_p measurements down to 1.8 K for all values of x except for $x = 1$, we reasonably assume that when doping ACC with K^+ ions, the crystallographic structure does not deviate from the room temperature structure. Additionally, because all of the mixed compositions had a detectable Δ , we propose a model similar to that proposed by Oosawa and Tanaka [40]. In it, the field-induced phase transition in KCC is described by the Bose-Einstein condensation (BEC) of excited triplets. The partial substitution of the K^+ ion for the NH_4^+ ion produces randomness for interactions between the Cu^{2+} ions, and hence the magnons. Up to a certain substitution level, the magnitude of the randomness may increase with increasing x , which is expressed in terms of the chemical potential of the magnon, $\mu = g\mu_B(H - H_g)$ [64].

As already mentioned, $g\mu_B H$ can be expressed in terms of the inter and intradimer exchange constants J' and J , respectively. Inelastic neutron scattering experiments have shown that for KCC, the susceptibility is dominated by an average intradimer $J = 49.9$ K [27,28]. On the other hand, J for ACC is markedly lower for all directions, with $J_A = 3.5$ K, $J_B = 20.9$ K, and $J_C = 34.8$ K [15]. This difference in interaction for each site is represented by differences in potential $\delta\mu_i$ for each dimer site i ; similar arguments can be made for the interdimer exchange constants. The net result is that the BEC is suppressed, such that the transition temperature and Δ decreases with increasing x . Further modeling would especially prove to be useful since a wide range of concentrations were covered in our experiments, which is further emphasized with the heightened sensitivity of Δ with x from $0.9 < x < 1.0$.

ACKNOWLEDGMENT

The authors would like to thank the Lawton Foundation of FSU for their support.

-
- [1] J. S. Kinyon, R. Clark, N. S. Dalal, E. S. Choi, and H. Zhou, Ferroelectricity in the gapless quantum antiferromagnet NH_4CuCl_3 , *Phys. Rev. B* **92**, 144103 (2015).
- [2] J. S. Kinyon, R. Clark, N. S. Dalal, and E. S. Choi, Magneto-electric coupling in the gapless NH_4CuCl_3 , *Ferroelectrics* **534**, 159 (2018).
- [3] W. Shiramura, K. ichi Takatsu, B. Kurniawan, H. Tanaka, H. Uekusa, Y. Ohashi, K. Takizawa, H. Mitamura, and T. Goto, Magnetization plateaus in NH_4CuCl_3 , *J. Phys. Soc. Jpn.* **67**, 1548 (1998).
- [4] R. D. Willett, J. Claudius Dwiggin, R. F. Kruh, and R. E. Rundle, Crystal structures of $KCuCl_3$ and NH_4CuCl_3 , *J. Chem. Phys.* **38**, 2429 (1963).
- [5] G. O'Bannon and R. D. Willet, A redetermination of the crystal structure of NH_4CuCl_3 and a magnetic study of NH_4CuX_3 ($x = Cl, Br$), *Inorg. Chim. Acta* **53**, L131 (1981).
- [6] T. Tonegawa, T. Nishida, and M. Kaburagi, Ground-state magnetization curve of a generalized spin-1/2 ladder, *Phys. B: Condens. Matter* **246–247**, 368 (1998).
- [7] K. Totsuka, Magnetization plateau in the $s = \frac{1}{2}$ Heisenberg spin chain with next-nearest-neighbor and alternating nearest-neighbor interactions, *Phys. Rev. B* **57**, 3454 (1998).
- [8] M. Oshikawa, M. Yamanaka, and I. Affleck, Magnetization Plateaus in Spin Chains: "Haldane Gap" for Half-Integer Spins, *Phys. Rev. Lett.* **78**, 1984 (1997).
- [9] M. Matsumoto, Microscopic model for the magnetization plateaus in NH_4CuCl_3 , *Phys. Rev. B* **68**, 180403(R) (2003).
- [10] A. Heyns and C. Schutte, Low-temperature infrared studies: VII. The infrared spectrum of and possible antiferromagnetic transition in ammonium trichlorocuprate NH_4CuCl_3 , *J. Mol. Struct.* **8**, 339 (1971).
- [11] S. Schmidt, S. Zherlitsyn, B. Wolf, H. Schwenk, B. Lüthi, and H. Tanaka, Phonon effects and ESR in NH_4CuCl_3 , *Europhys. Lett.* **54**, 554 (2001).
- [12] B. Lüthi, B. Wolf, S. Zherlitsyn, S. Schmidt, H. Schwenk, and M. Sieling, Pulsed field ultrasonic and ESR experiments in low-dimensional spin systems, *Physica B* **294**, 20 (2001).
- [13] Y. Shimaoka, T. Goto, K. Kodama, M. Takigawa, and H. Tanaka, NMR study of magnetic structures in NH_4CuCl_3 , *Physica B* **329–333**, 894 (2003).
- [14] K. Kodama, M. Takigawa, and H. Tanaka, Structural transitions and magnetic structure in NH_4CuCl_3 via ^{14}N -NMR, *Prog. Theor. Phys. Suppl.* **159**, 228 (2005).
- [15] C. Rüegg, M. Oettli, J. Schefer, O. Zaharko, A. Furrer, H. Tanaka, K. W. Krämer, H. U. Güdel, P. Vorderwisch, K. Habicht, T. Polinski, and M. Meissner, Neutron Scattering Study of the Field-Dependent Ground State and the Spin Dynamics in Spin-One-Half NH_4CuCl_3 , *Phys. Rev. Lett.* **93**, 037207 (2004).
- [16] A. Oosawa, T. Ono, K. Kakurai, and H. Tanaka, Magnetic excitations in the quantum spin system NH_4CuCl_3 , [arXiv:cond-mat/0304172](https://arxiv.org/abs/cond-mat/0304172).
- [17] M. Matsumoto, B. Normand, T. M. Rice, and M. Sigrist, Magnon dispersion in field-induced magnetically ordered phases, *J. Magn. Magn. Mater.* **272–276**, 267 (2004).
- [18] H. Inoue, S. Tani, S. Hosoya, K. Inokuchi, T. Fujiwara, T. Saito, T. Suzuki, A. Oosawa, T. Goto, M. Fujisawa, H. Tanaka, T. Sasaki, S. Awaji, K. Watanabe, and N. Kobayashi, $^{63/65}Cu$ and $^{35/37}Cl$ -NMR studies of triplet localization in the quantum spin system NH_4CuCl_3 , *Phys. Rev. B* **79**, 174418 (2009).
- [19] S.-i. Tani, H. Inoue, T. Suzuki, S. Hosoya, K. Inokuchi, T. Fujiwara, T. Goto, H. Tanaka, T. Sasaki, S. Awaji, K. Watanabe, and N. Kobayashi, Cu-NMR study on field-induced phase transitions in quantum spin magnet NH_4CuCl_3 , *Prog. Theor. Phys. Suppl.* **159**, 235 (2005).
- [20] S. Hosoya, K. Inokuchi, T. Suzuki, T. Goto, H. Tanaka, S. Awaji, K. Watanabe, T. Sasaki, T. Fukase, T. Shimizu, and A. Goto, NMR study on the quantum spin ladder NH_4CuCl_3 , *Physica B* **329**, 977 (2003).
- [21] B. Kurniawan, H. Tanaka, K. Takatsu, W. Shiramura, T. Fukuda, H. Nojiri, and M. Motokawa, ESR Study of the Opening and Closing of the Field-Induced Gap in NH_4CuCl_3 , *Phys. Rev. Lett.* **82**, 1281 (1999).

- [22] H. Nojiri, H. Tanaka, B. Kurniawan, and M. Motokawa, Coexistence of gap-less and gapped excitations in NH_4CuCl_3 , *Physica B* **329**, 701 (2003).
- [23] B. Kurniawan, M. Ishikawa, T. Kato, H. Tanaka, K. Takizawa, and T. Goto, Novel three-dimensional magnetic ordering in the quantum spin system NH_4CuCl_3 , *J. Phys.: Condens. Matter* **11**, 9073 (1999).
- [24] H. Tanaka, K. ichi Takatsu, W. Shiramura, and T. Ono, Singlet ground state and excitation gap in the double spin chain system KCuCl_3 , *J. Phys. Soc. Jpn.* **65**, 1945 (1996).
- [25] A. Oosawa, T. Takamasu, K. Tatani, H. Abe, N. Tsujii, O. Suzuki, H. Tanaka, G. Kido, and K. Kindo, Field-induced magnetic ordering in the quantum spin system KCuCl_3 , *Phys. Rev. B* **66**, 104405 (2002).
- [26] K. Kakurai, M. Nishi, K. Nakajima, K. Nukui, N. Aso, T. Kato, H. Tanaka, H. Kageyama, Y. Ueda, L. P. Regnault, B. Grenier, and B. Fok, Neutron scattering experiments on low-dimensional quantum spin systems—spin excitations in KCuCl_3 and $\text{SrCu}_2(\text{BO}_3)_2$, *J. Phys. Chem. Solids* **62**, 141 (2001).
- [27] N. Cavadini, G. Heigold, W. Henggeler, A. Furrer, H. U. Güdel, K. Krämer, and H. Mutka, Quantum magnetic interactions in $S = 1/2\text{KCuCl}_3$, *J. Phys.: Condens. Matter* **12**, 5463 (2000).
- [28] N. Cavadini, W. Henggeler, A. Furrer, H. U. Güdel, K. Krämer, and H. Mutka, Magnetic excitations in the quantum spin system KCuCl_3 , *Eur. Phys. J. B* **7**, 519 (1999).
- [29] N. Cavadini, W. Henggeler, A. Furrer, H. U. Güdel, K. Krämer, and H. Mutka, Magnetic excitations and spin gap in KCuCl_3 , *Physica B* **276–278**, 540 (2000).
- [30] T. Kato, K.-i., Takatsu, H. Tanaka, W. Shiramura, M. Mori, K. Nakajima, and K. Kakurai, Magnetic excitations in the spin gap system KCuCl_3 , *J. Phys. Soc. Jpn.* **67**, 752 (1998).
- [31] T. Kato, A. Oosawa, K. Takatsu, H. Tanaka, W. Shiramura, K. Nakajima, and K. Kakurai, Magnetic excitations in the spin gap system KCuCl_3 and TlCuCl_3 , *J. Phys. Chem. Solids* **60**, 1125 (1999).
- [32] K. Goto, M. Fujisawa, A. Oosawa, T. Osakabe, K. Kakurai, Y. Uwatoko, and H. Tanaka, Pressure-induced magnetic quantum phase transition in KCuCl_3 , *J. Phys. Soc. Jpn.* **76**, 162 (2007).
- [33] K. Goto, T. Osakabe, K. Kakurai, Y. Uwatoko, A. Oosawa, J. Kawakami, and H. Tanaka, Softening of magnetic excitations leading to pressure-induced quantum phase transition in gapped spin system KCuCl_3 , *J. Phys. Soc. Jpn.* **76**, 053704 (2007).
- [34] K. Goto, T. Osakabe, K. Kakurai, Y. Uwatoko, A. Oosawa, J. Kawakami, and H. Tanaka, Erratum: Softening of magnetic excitations leading to pressure-induced quantum phase transition in gapped spin system KCuCl_3 , *J. Phys. Soc. Jpn.* **76**, 098002 (2007).
- [35] K. Goto, M. Fujisawa, H. Tanaka, Y. Uwatoko, A. Oosawa, T. Osakabe, and K. Kakurai, Pressure-induced magnetic quantum phase transition in gapped spin system KCuCl_3 , *J. Phys. Soc. Jpn.* **75**, 064703 (2006).
- [36] K. Goto, M. Fujisawa, H. Tanaka, Y. Uwatoko, A. Oosawa, T. Osakabe, and K. Kakurai, Erratum: Pressure-induced magnetic quantum phase transition in gapped spin system KCuCl_3 , *J. Phys. Soc. Jpn.* **76**, 098001 (2007).
- [37] H. Tanaka, T. Takatsu, W. Shiramura, T. Kambe, H. Nojiri, T. Yamada, S. Okubo, H. Ohta, and M. Motokawa, High-frequency high-field ESR of quantum double spin chain systems KCuCl_3 and TlCuCl_3 , *Physica B* **246–247**, 545 (1998).
- [38] Müllerand H.-J. Mikeska, On the dynamics of coupled $S = 1/2$ antiferromagnetic zigzag chains, *J. Phys.: Condens. Matter* **12**, 7633 (2000).
- [39] T. Suzuki, F. Yamada, I. Watanabe, T. Goto, A. Oosawa, and H. Tanaka, Bond-randomness effect on the quantum spin system probed by muon-spin-relaxation method, *Physica B: Condens. Matter* **404**, 590 (2009).
- [40] A. Oosawa and H. Tanaka, Random bond effect in the quantum spin system $\text{Tl}_{(1-x)}\text{K}_x\text{CuCl}_3$, *Phys. Rev. B* **65**, 184437 (2002).
- [41] N. Cavadini, G. Heigold, W. Henggeler, A. Furrer, H. U. Güdel, K. Krämer, and H. Mutka, Magnetic excitations in the quantum spin system TlCuCl_3 , *Phys. Rev. B* **63**, 172414 (2001).
- [42] A. Oosawa, M. Ishii, and H. Tanaka, Field-induced three-dimensional magnetic ordering in the spin-gap system, *J. Phys.: Condens. Matter* **11**, 265 (1999).
- [43] H. Tanaka, A. Oosawa, T. Kato, H. Uekusa, Y. Ohashi, K. Kakurai, and A. Hoser, Observation of field-induced transverse neél ordering in the spin gap system TlCuCl_3 , *J. Phys. Soc. Jpn.* **70**, 939 (2001).
- [44] W. Shiramura, K.-i. Takatsu, H. Tanaka, K. Kamishima, M. Takahashi, H. Mitamura, and T. Goto, High-field magnetization processes of double spin chain systems KCuCl_3 and TlCuCl_3 , *J. Phys. Soc. Jpn.* **66**, 1900 (1997).
- [45] K.-i. Takatsu, W. Shiramura, and H. Tanaka, Ground states of double spin chain systems TlCuCl_3 , NH_4CuCl_3 and KCuBr_3 , *J. Phys. Soc. Jpn.* **66**, 1611 (1997).
- [46] T. Suzuki, M. Yamada, Y. Ishii, I. Watanabe, T. Goto, H. Tanaka, and K. Kubo, Change in magnetic ground states in nonmagnetic-impurity-doped spin-gap systems $\text{TlCu}_{1-x}\text{Mg}_x\text{Cl}_3$ using muon spin relaxation, *Phys. Rev. B* **83**, 174436 (2011).
- [47] M. Groger, *Z. Anorg. Chem.* **19**, 328 (1899).
- [48] J. Kinyon, Mixed trichlorocuprates: A new family of multiferroics, Ph.D. thesis, Florida State University, 2012.
- [49] P. Schiffer and I. Daruka, Two-population model for anomalous low-temperature magnetism in geometrically frustrated magnets, *Phys. Rev. B* **56**, 13712 (1997).
- [50] R. Siddharthan, B. S. Shastry, A. P. Ramirez, A. Hayashi, R. J. Cava, and S. Rosenkranz, Ising Pyrochlore Magnets: Low-Temperature Properties, “Ice Rules,” and Beyond, *Phys. Rev. Lett.* **83**, 1854 (1999).
- [51] K. D. Bleaney, Brebisand Bowers, Anomalous paramagnetism of copper acetate, *Proc. R. Soc. A* **214**, 451 (1952).
- [52] A. A. Aczel, Y. Kohama, C. Marcenat, F. Weickert, M. Jaime, O. E. Ayala-Valenzuela, R. D. McDonald, S. D. Selesnic, H. A. Dabkowska, and G. M. Luke, Field-Induced Bose-Einstein Condensation of Triplons up to 8 K in $\text{Sr}_3\text{Cr}_2\text{O}_8$, *Phys. Rev. Lett.* **103**, 207203 (2009).
- [53] K. ichi Hara, M. Inoue, S. Emori, and M. Kubo, Magnetic interaction between binuclear clusters in potassium trihalocuprates(II) and dimethylammonium trihalocuprates(II), *J. Magn. Reson.* (1969) **4**, 337 (1971).
- [54] M. Troyer, H. Tsunetsugu, and D. Würtz, Thermodynamics and spin gap of the Heisenberg ladder calculated by the look-ahead Lanczos algorithm, *Phys. Rev. B* **50**, 13515 (1994).
- [55] A. Oosawa, H. A. Katori, and H. Tanaka, Specific heat study of the field-induced magnetic ordering in the spin-gap system TlCuCl_3 , *Phys. Rev. B* **63**, 134416 (2001).
- [56] T. Besara, P. Jain, N. S. Dalal, P. L. Kuhns, A. P. Reyes, H. W. Kroto, and A. K. Cheetham, Mechanism of the order–disorder

- phase transition, and glassy behavior in the metal-organic framework $[(\text{CH}_3)_2\text{NH}_2]\text{Zn}(\text{HCOO})_3$, *Proc. Natl. Acad. Sci. USA* **108**, 6828 (2011)
- [57] B. C. Melot, R. Tackett, J. O'Brien, A. L. Hector, G. Lawes, R. Seshadri, and A. P. Ramirez, Large low-temperature specific heat in pyrochlore $\text{Bi}_2\text{Ti}_2\text{O}_7$, *Phys. Rev. B* **79**, 224111 (2009).
- [58] C. A. Angell, Formation of glasses from liquids and biopolymers, *Science* **267**, 1924 (1995).
- [59] V. Lubchenko and P. G. Wolynes, The origin of the boson peak and thermal conductivity plateau in low-temperature glasses, *Proc. Natl. Acad. Sci. USA* **100**, 1515 (2003).
- [60] H. Shintani and H. Tanaka, Universal link between the boson peak and transverse phonons in glass, *Nat. Mater.* **7**, 870 (2008).
- [61] D. J. Safarik, R. B. Schwarz, and M. F. Hundley, Similarities in the C_p/T^3 Peaks in Amorphous and Crystalline Metals, *Phys. Rev. Lett.* **96**, 195902 (2006).
- [62] K.-Y. Choi, A. Oosawa, H. Tanaka, and P. Lemmens, Interplay of triplets and lattice degrees of freedom in the coupled spin dimer system KCuCl_3 , *Phys. Rev. B* **72**, 024451 (2005).
- [63] K.-Y. Choi, A. Oosawa, H. Tanaka, and P. Lemmens, Inelastic light scattering experiments on the coupled spin dimer system $\text{Tl}_1 - x\text{K}_x\text{CuCl}_3$, *Prog. Theor. Phys. Suppl.* **159**, 195 (2005).
- [64] T. Nikuni, M. Oshikawa, A. Oosawa, and H. Tanaka, Bose-Einstein Condensation of Dilute Magnons in TlCuCl_3 , *Phys. Rev. Lett.* **84**, 5868 (2000).